

# Comparative study for inclusion complexes of nonsteroidal anti-inflammatory drugs with 2-hydroxypropyl- $\beta$ -cyclodextrins about their dissolution rate and supersaturation

Yukiko Oshite, Ayako Wada-Hirai, Risa Ichii, Chihiro Kuroda, Kanji Hasegawa, Ryosuke Hiroshige, Hideshi Yokoyama, Tomohiro Tsuchida and Satoru Goto\*  
Faculty of Pharmaceutical Sciences, Tokyo University of Science

## Supplemental Materials

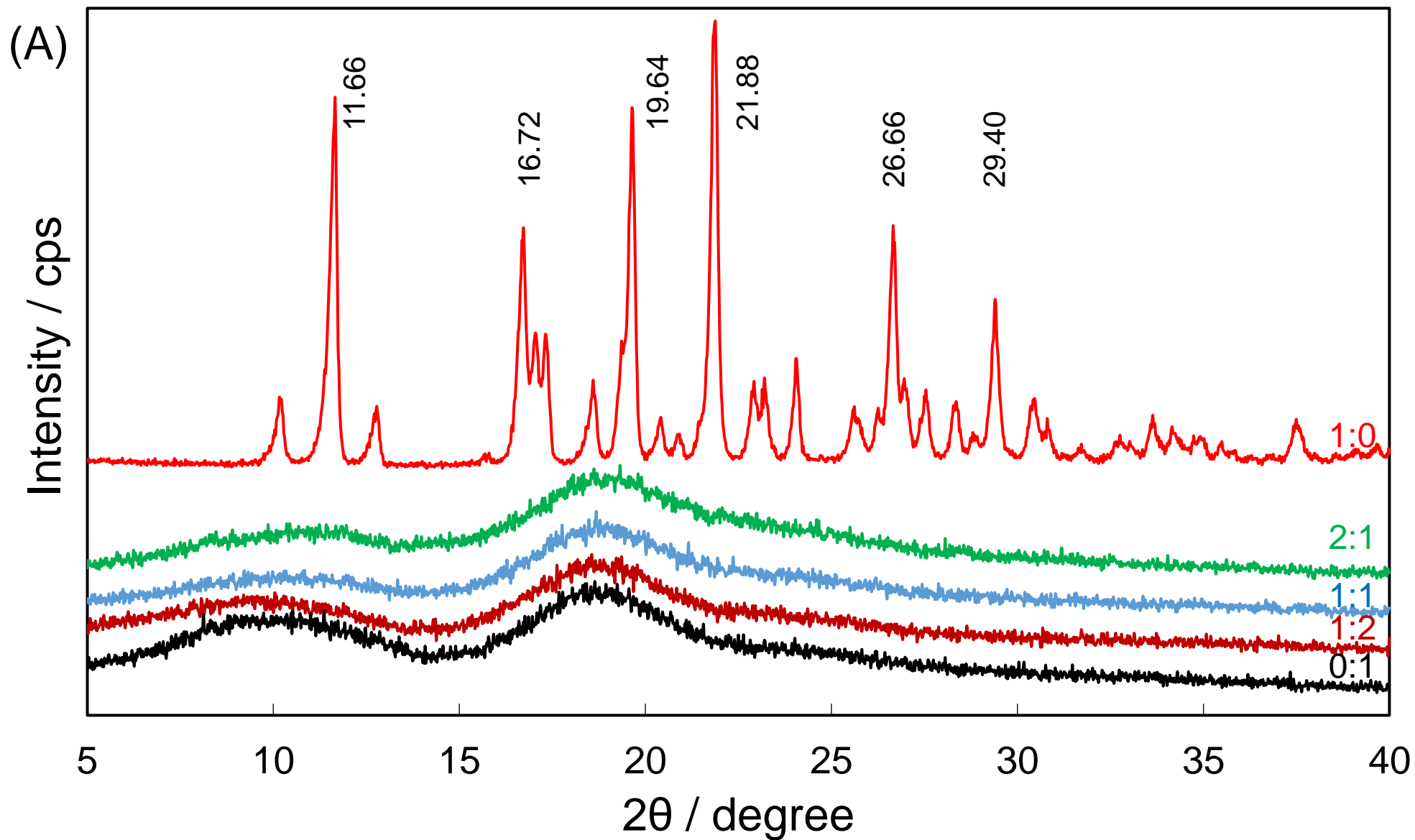


Figure S1 (A) The XRPD patterns of the neat INM (1:0, red), its mixtures with HP-β-CD at molar ratios of 2:1 (green), 1:1 (blue), and 1:2 (brown), and the plain HP-β-CD (0:1, black). The 2θ values represent close to conspicuous peaks.

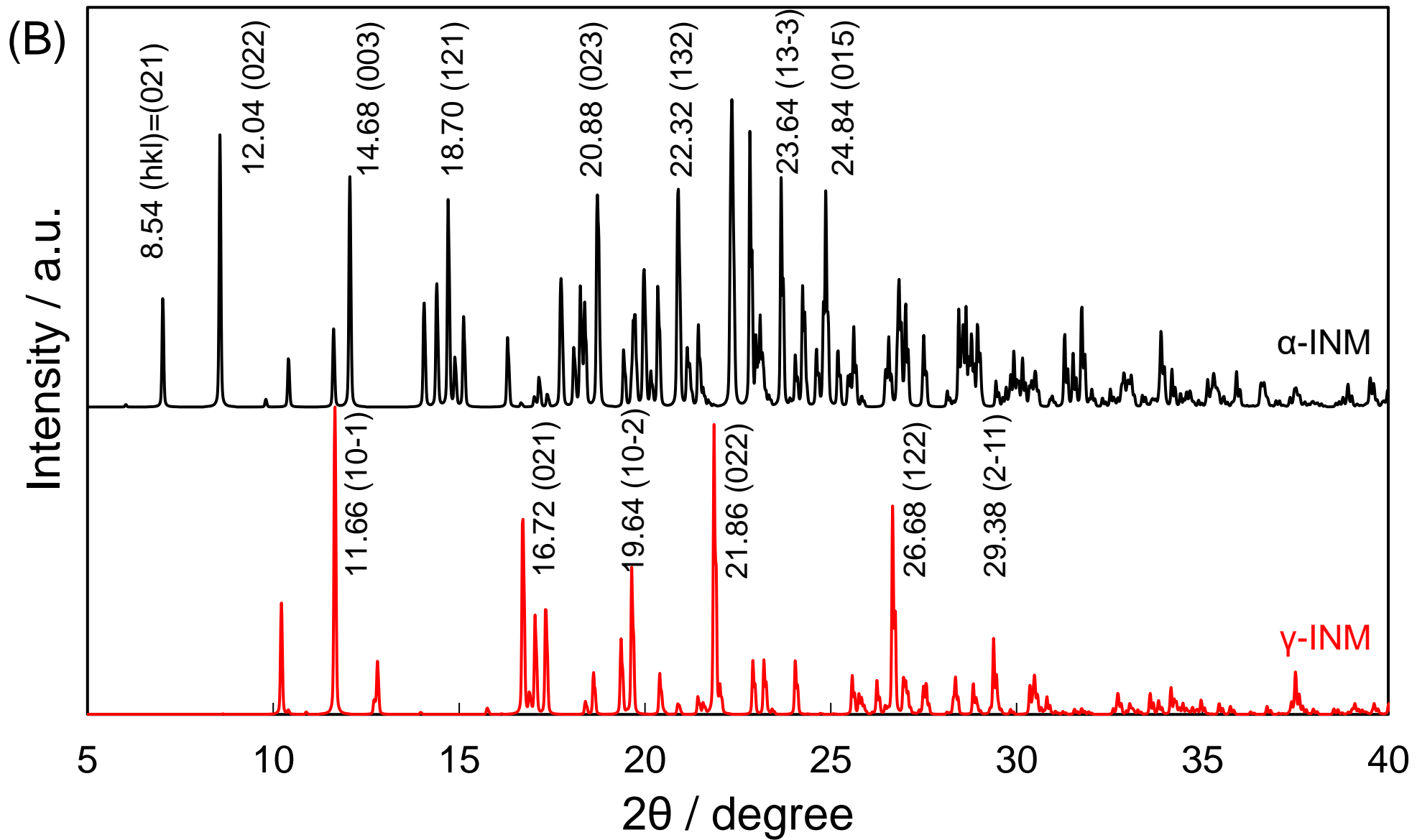


Figure S1 (B) The simulated diffractograms of  $\alpha$ - (black) and  $\gamma$ -INM (red). The corresponding CCDC entries are INDMET04 (M. Arisawa, et al 2011) and INDMET (T.J. Kistemacher & R.E. Marsh, 1972).

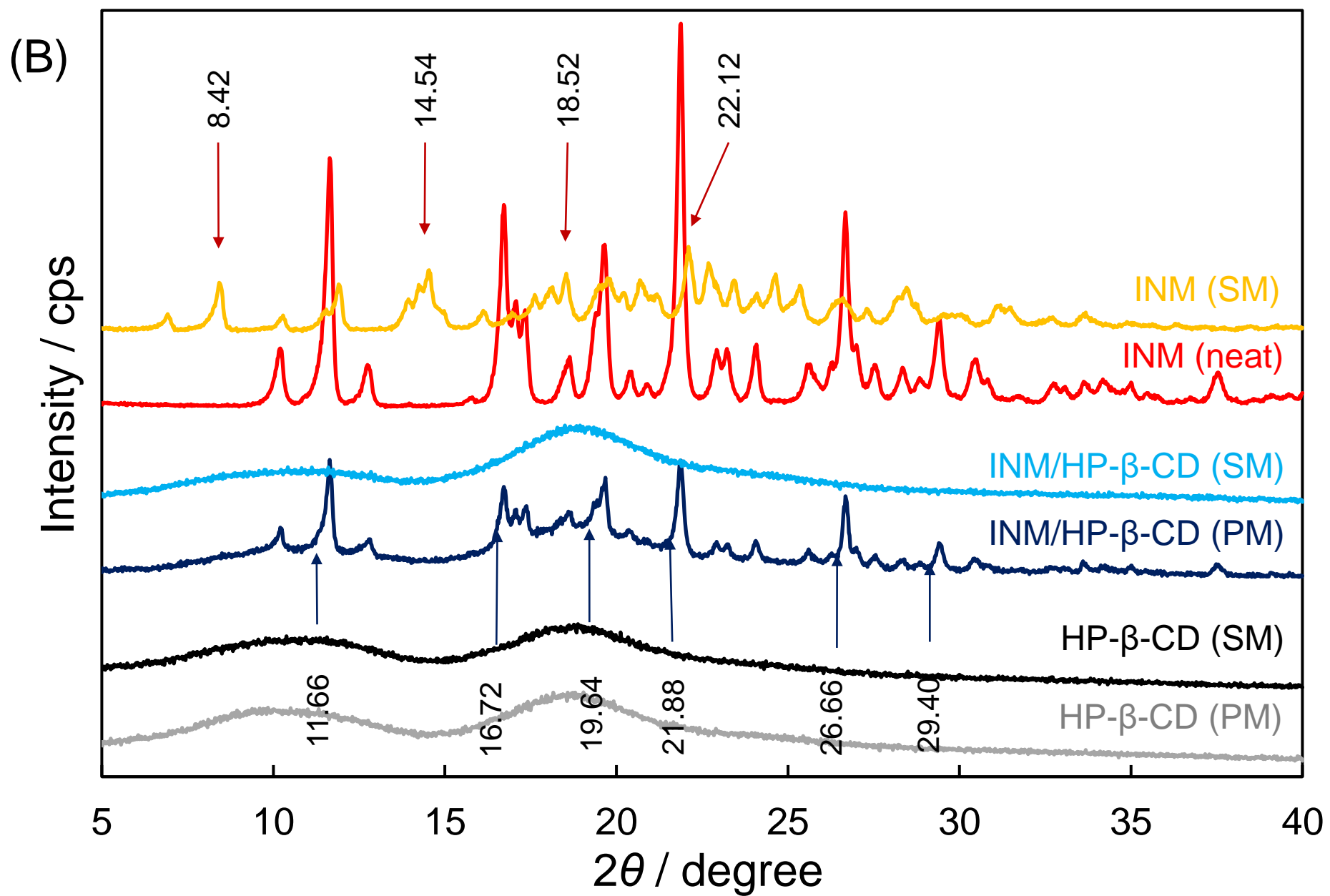


Figure S1(C) XRPD diffractograms of neat/SM-treated INM, the SM-/PM-prepared equimolar mixtures of INM and HP- $\beta$ -CD, and those of HP- $\beta$ -CD.

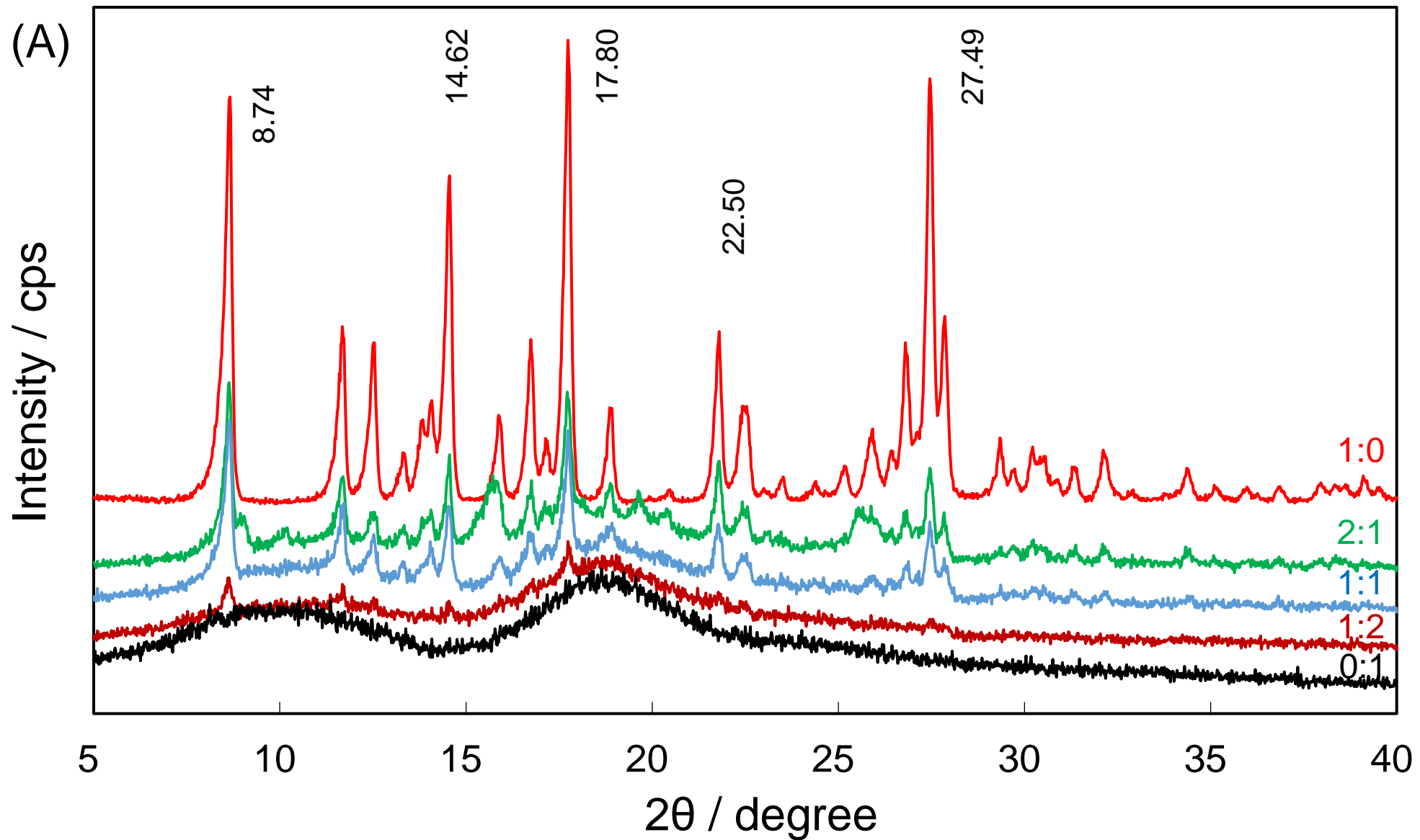


Figure S2 (A) The XRPD patterns of the neat PRX (1:0, red), its mixtures with HP- $\beta$ -CD at molar ratios of 2:1 (green), 1:1 (blue), and 1:2 (brown), and the plain HP- $\beta$ -CD (0:1, black). The  $2\theta$  values represent close to conspicuous peaks.

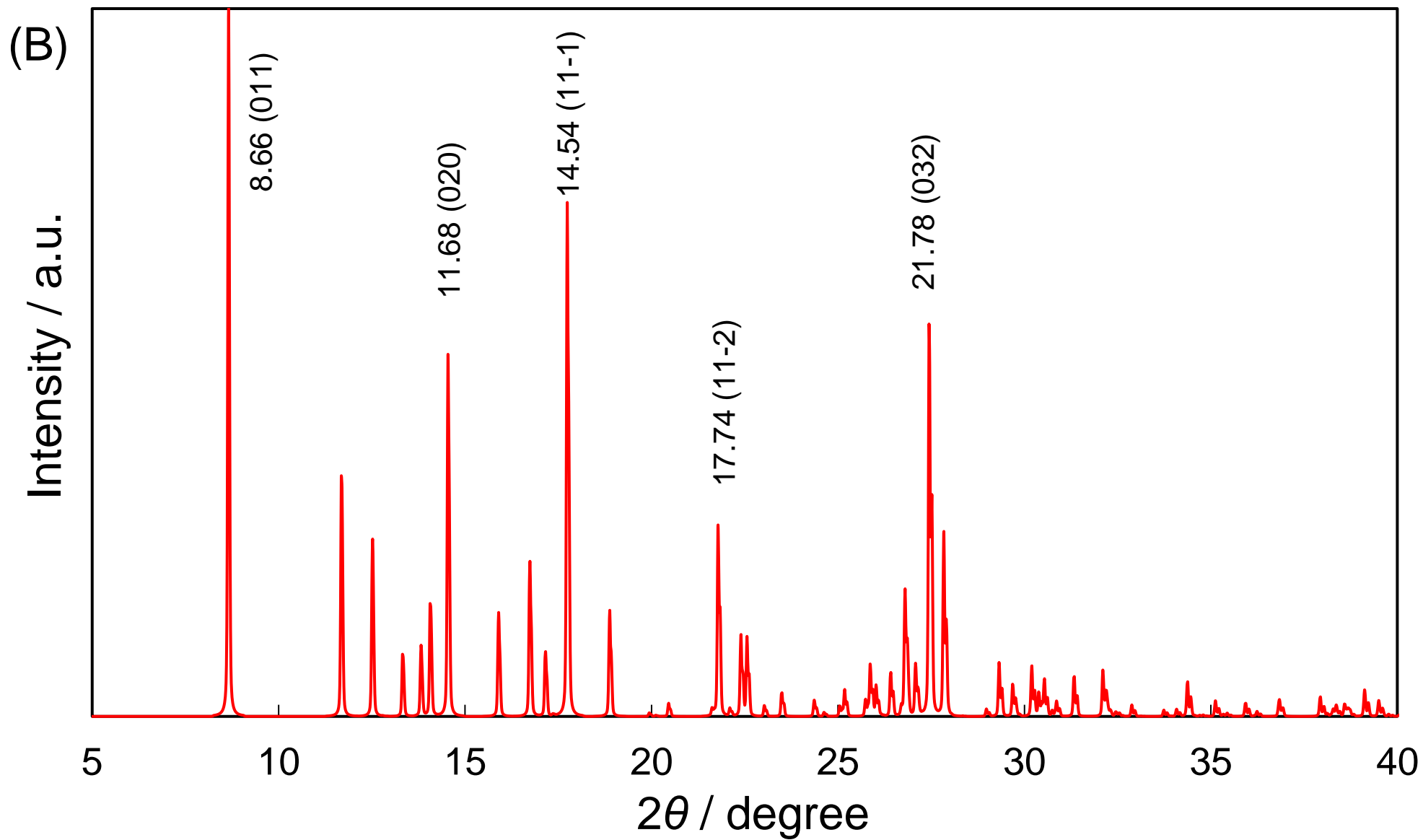


Figure S2 (B) The simulated diffractograms of PRX. The CCDC entry is BIYSEH (B. Kojic-Prodic & Z. Ruzic-Toros, 1982).

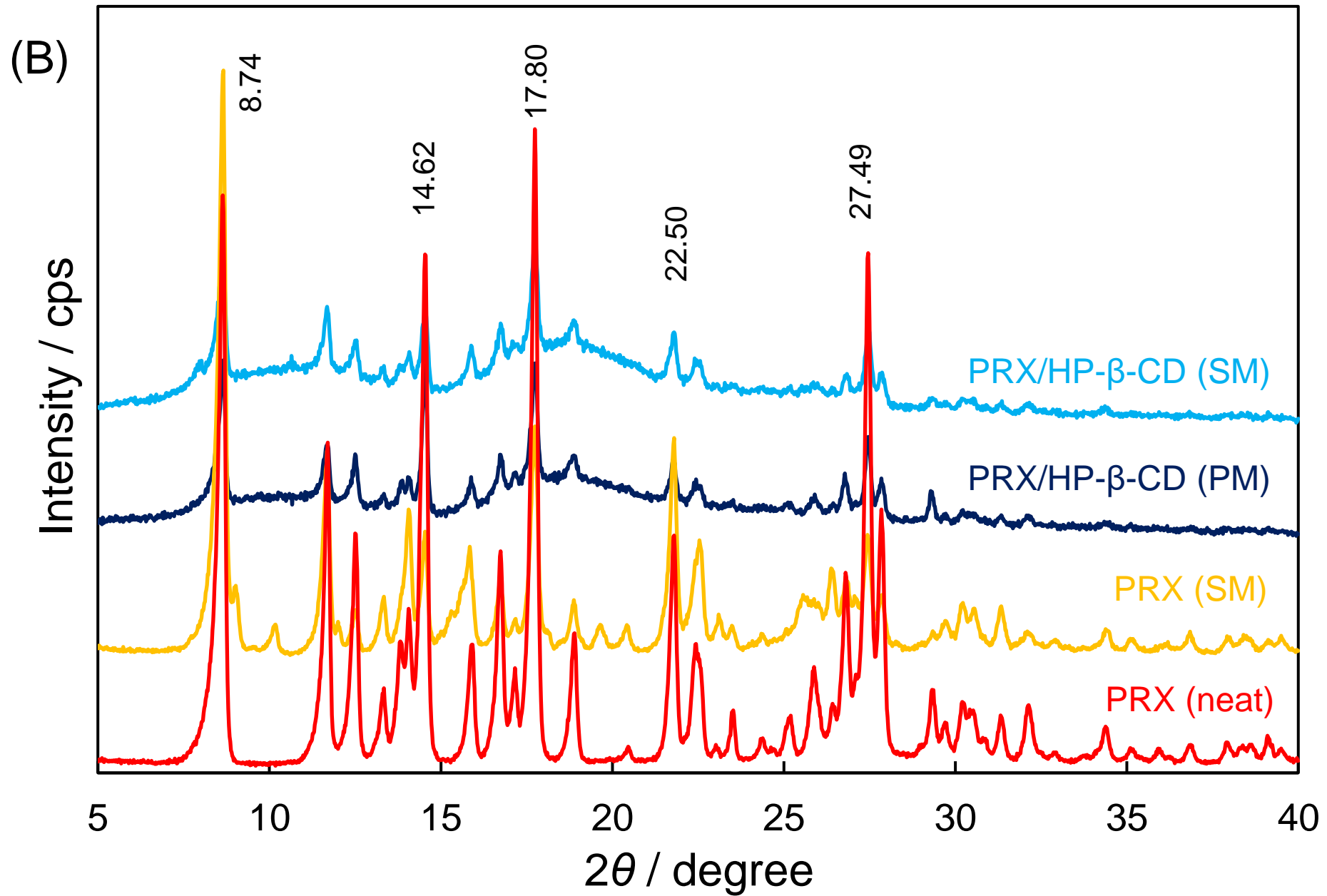


Figure S2(C) XRPD diffractograms of the neat/SM-treated PRX and the SM-/PM-prepared equimolar mixtures of PRX HP- $\beta$ -CD.

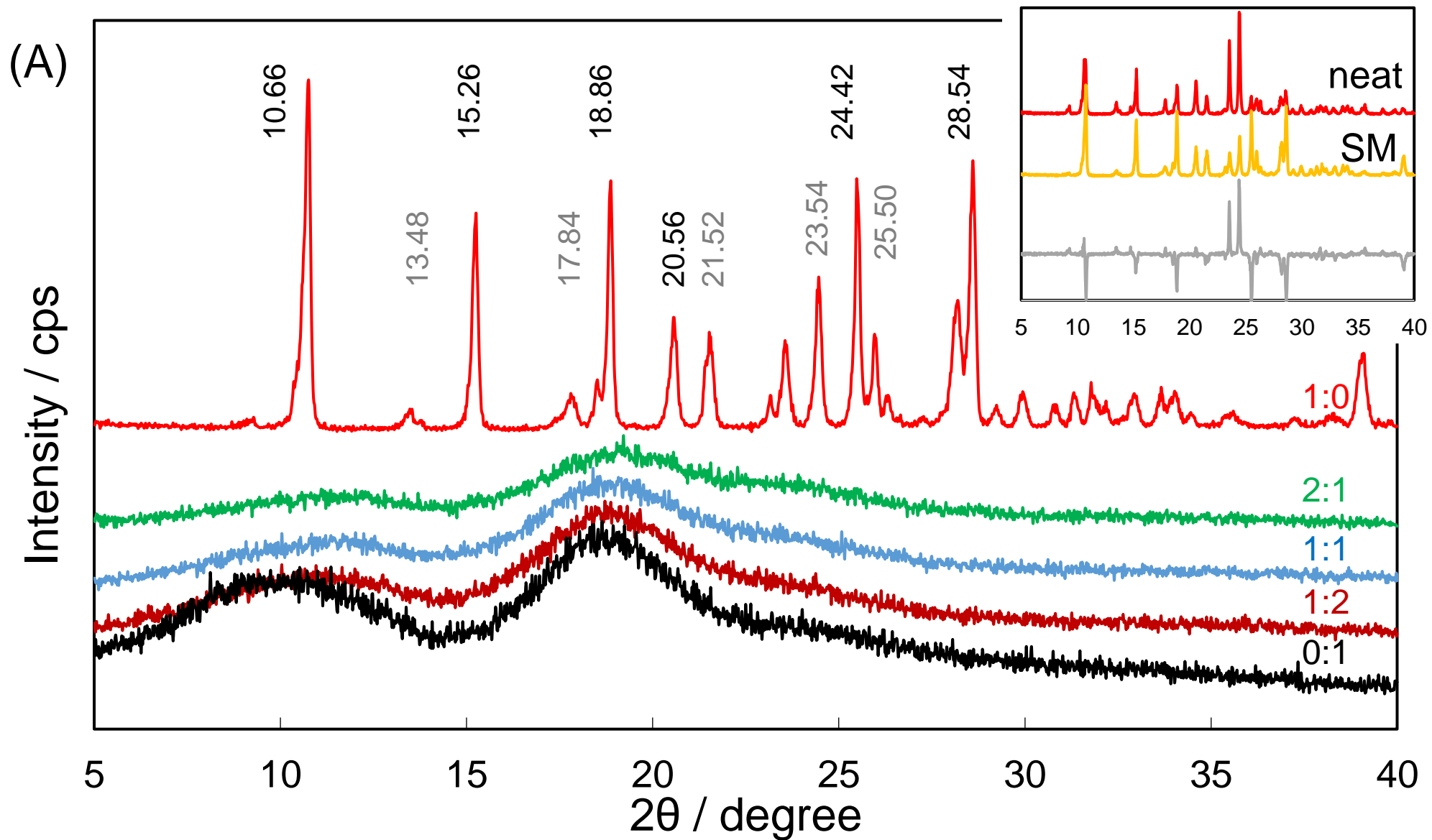


Figure S3 (A) The XRPD patterns of the neat DCF (1:0, red), its mixtures with HP- $\beta$ -CD at molar ratios of 2:1 (green), 1:1 (blue), and 1:2 (brown), and the plain HP- $\beta$ -CD (0:1, black). The  $2\theta$  values represent close to conspicuous peaks. The inset shows the difference (gray) between neat (red) and PM-prepared (recrystallized) DCF (orange), indicating their diffraction angles to be invariant.



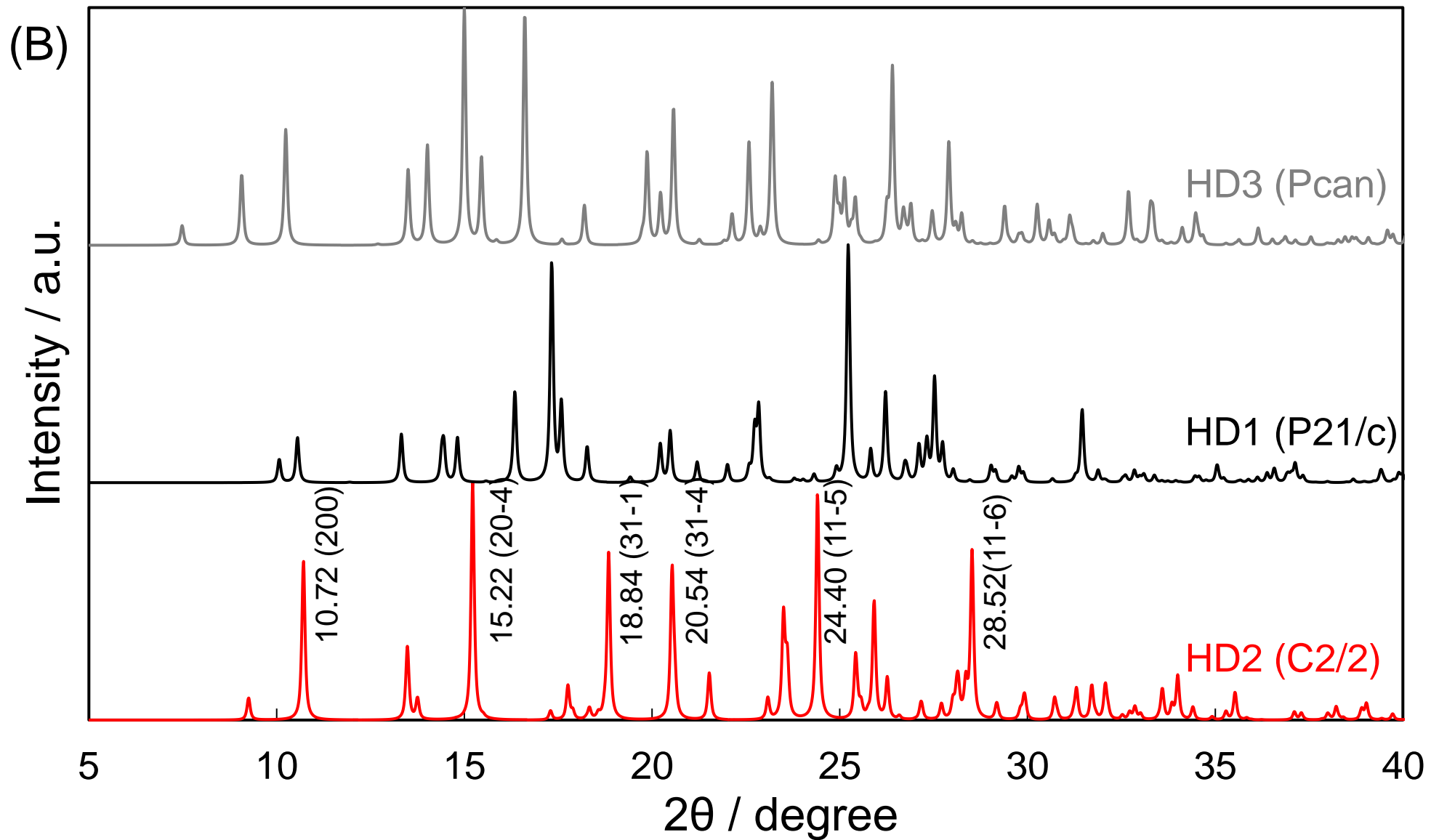


Figure S3 (B) The simulated diffractograms of DCF. The corresponding CCDC entries are SIKLIH (P. Moster, et al. 1990) for HD1 crystal, SIKLIH02 (C. Castellari & A. Ottani, 1997) for HD2, and SIKLIH04 (N. Jaiboon, et al. 2001) for HD3.

(B)

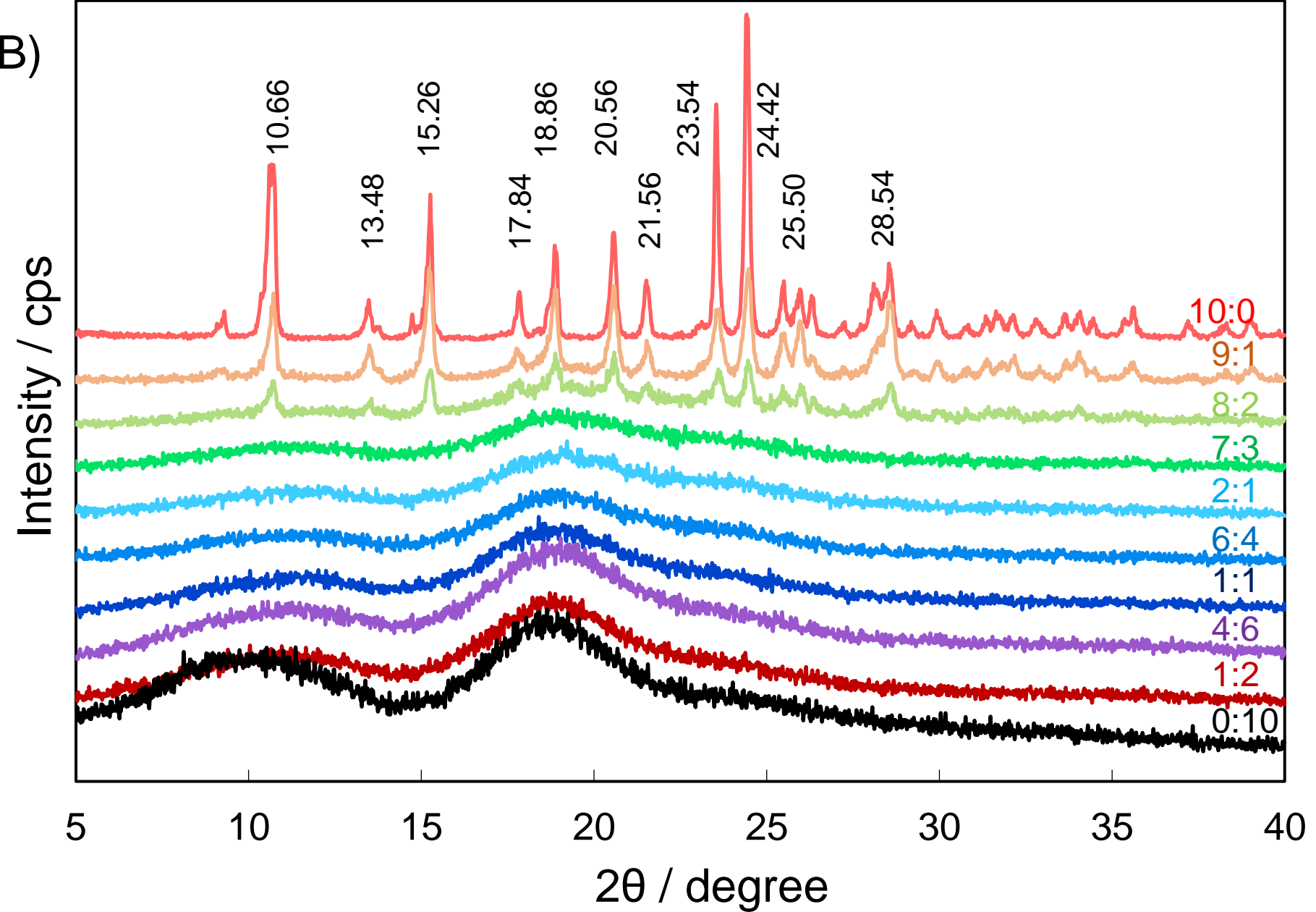


Figure S3(C) XRPD diffractograms of the SM-prepared mixtures of DCF and HP-β-CD at the various molar ratios.

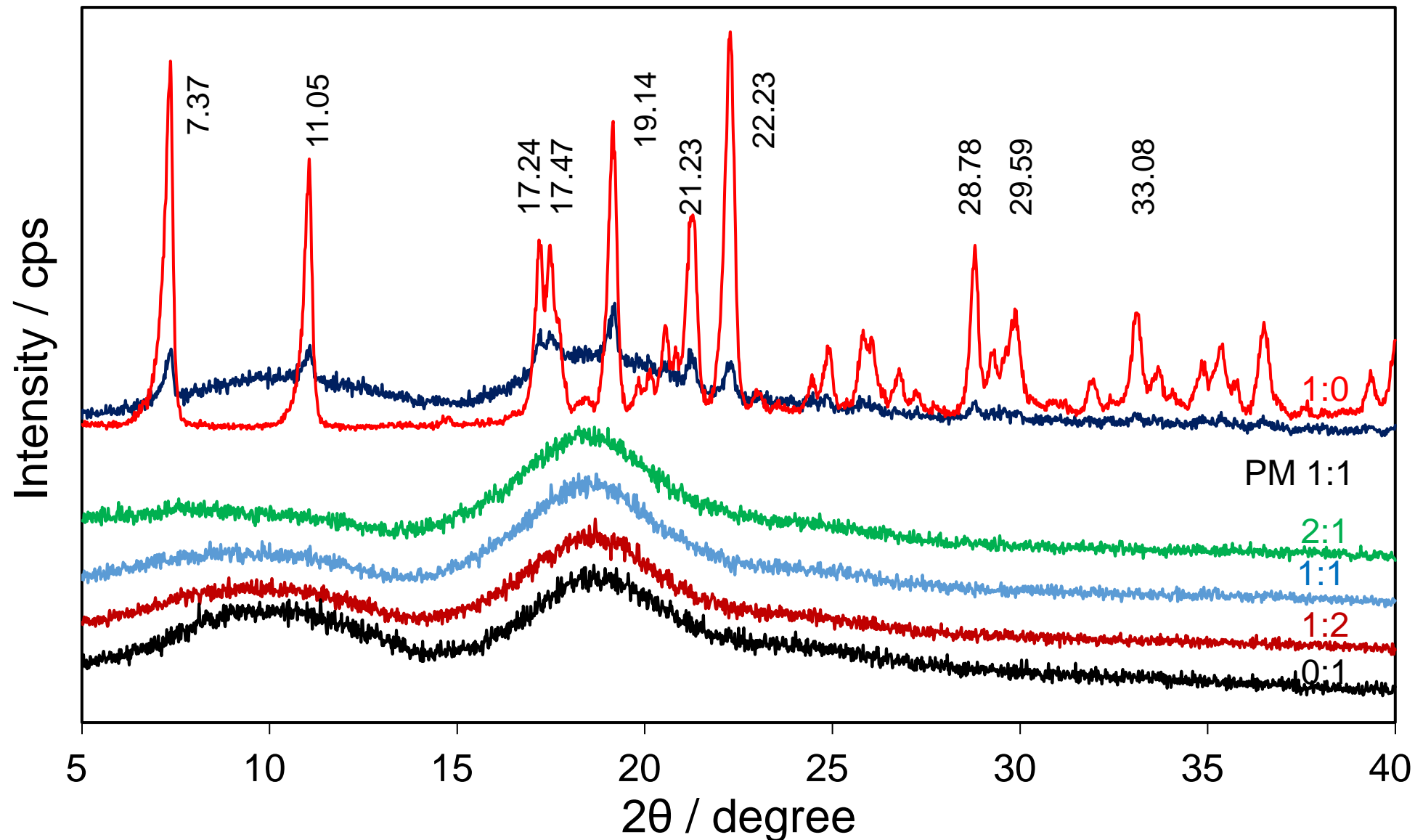


Figure S4 The XRPD patterns of the neat LXP-Na (1:0, red), its SM-prepared mixtures with HP- $\beta$ -CD at molar ratios of 2:1 (green), 1:1 (blue), and 1:2 (brown), the plain HP- $\beta$ -CD (0:1, black), and the PM-prepared equimolar mixture (indigo). The  $2\theta$  values represent close to conspicuous peaks.

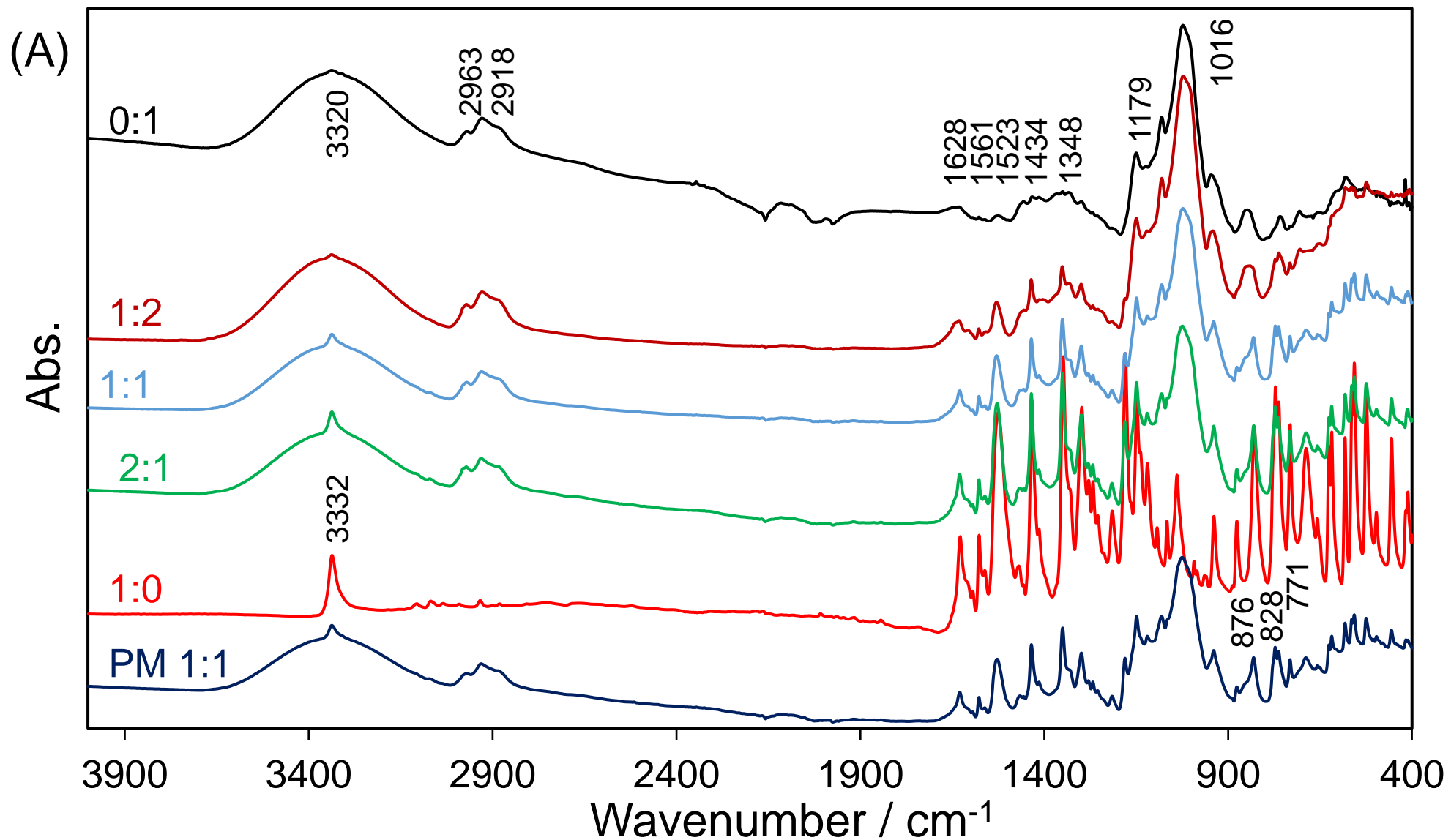
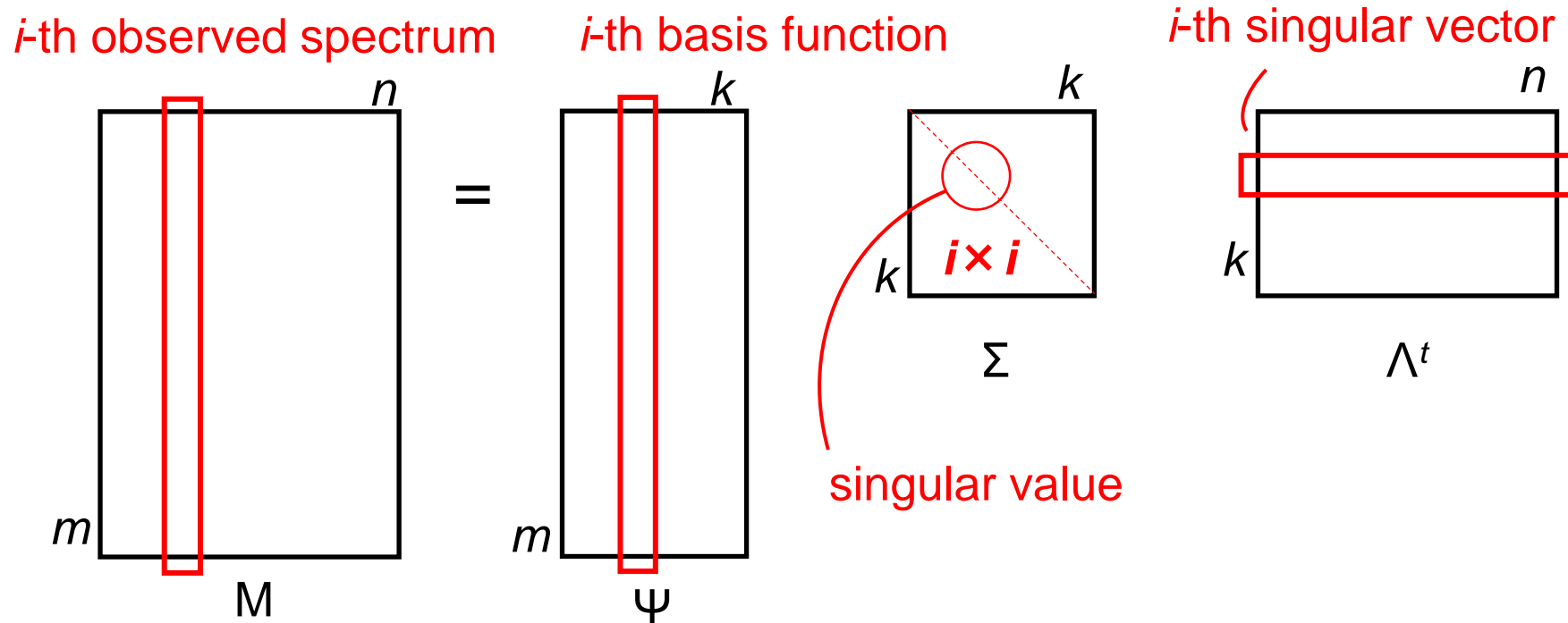


Figure S5(A) The ATR-FTIR spectra of the neat PRX (red), the plain HP- $\beta$ -CD (black), PM-prepared equimolar mixture (indigo), and SM-prepared mixtures at the molar ratios of 2:1 (green), 1:1 (blue), and 1:2 (brown). Each spectrum in the wavenumber range of 1800-400 cm<sup>-1</sup> is used for the following analysis.

The singular value decomposition (SVD) procedure for a spectroscopic dataset in Figure S5(A): The obtained spectra are considered to be linear combinations of the latent ones for unknown molecular compositions. For the experimental conditions expected to contribute linear combination coefficients, the spectral vectors are combined in order of the conditions as a matrix  $M$ . Due to the SVD procedure, the  $M$  is decomposed to be the basis function matrix  $\Psi$ , the diagonal matrix  $\Sigma$  of singular values, and the transposed matrix  $\Lambda^t$  of singular vectors:



where the  $i$ -th elemental vector in the  $\Psi$  matrix indicates one of the latent spectra for the assumed compositions. The  $i$ -th singular value in the  $\Sigma$  indicates the statistical variance in the contribution of the corresponding composition. The  $j$ -th singular vector in the  $\Lambda^t$  corresponds to the description vector to reproduce each observed spectrum with the basis functions and the singular values. The detail of the mathematical protocol for the SVD procedure was described in our previous papers. [41,42]

In the present study, the SVD analysis of FTIR of PRX mixtures indicated to be found the combined ones of PRX and HP- $\beta$ -CD, as described here. On nuclear magnetic resonance (NMR) spectroscopy, even if no cross-peaks were shifted, diminished, or enhanced corresponding to the interactions, it cannot indicate to deny the existence of the intermolecular interaction between PRX and HP- $\beta$ -CD. The NMR signal change would appear or disappear dependent on not presence or absence but the structural orientations of the interacting groups. Only if the NMR cross-peaks change, then we can confirm the interaction. It is the reason why NMR spectroscopy is meaningless here.

Suppose any API and HP- $\beta$ -CD form an inclusion complex or other intermolecular interaction, we consider that the FTIR spectra of their mixture contain a spectral component resembling neither those of the neat API nor plain HP- $\beta$ -CD with strong possibility. Practically, the SVD analyses for the mixtures of INM gave evidence that the third component was produced via the SM-prepared mixture of INM and HP- $\beta$ -CD, being different from INM and HP- $\beta$ -CD. The third component should correspond to that with the endothermic peaks at a lower temperature than the neat and SM-treated INM samples. We believe that the reproduced spectra of this component had better be verified their signals to be assigned structural rearrangements to form the third component as INM/HP- $\beta$ -CD inclusion complex. As insufficient evidence for that has been obtained yet, further observations are not described here and the present authors are going to write and submit a subsequent report.

A similar situation was observed for the DCF mixtures with HP- $\beta$ -CD.

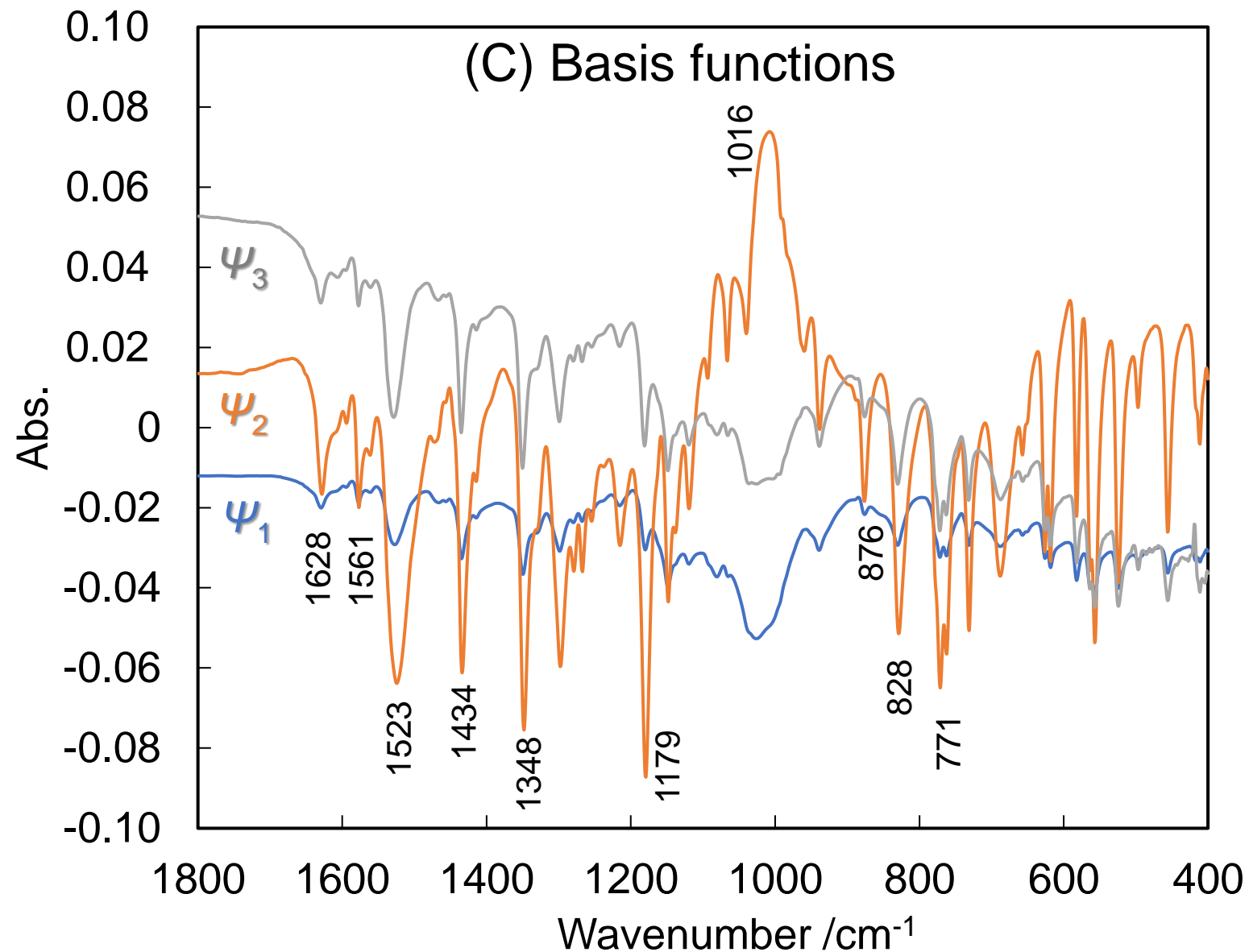
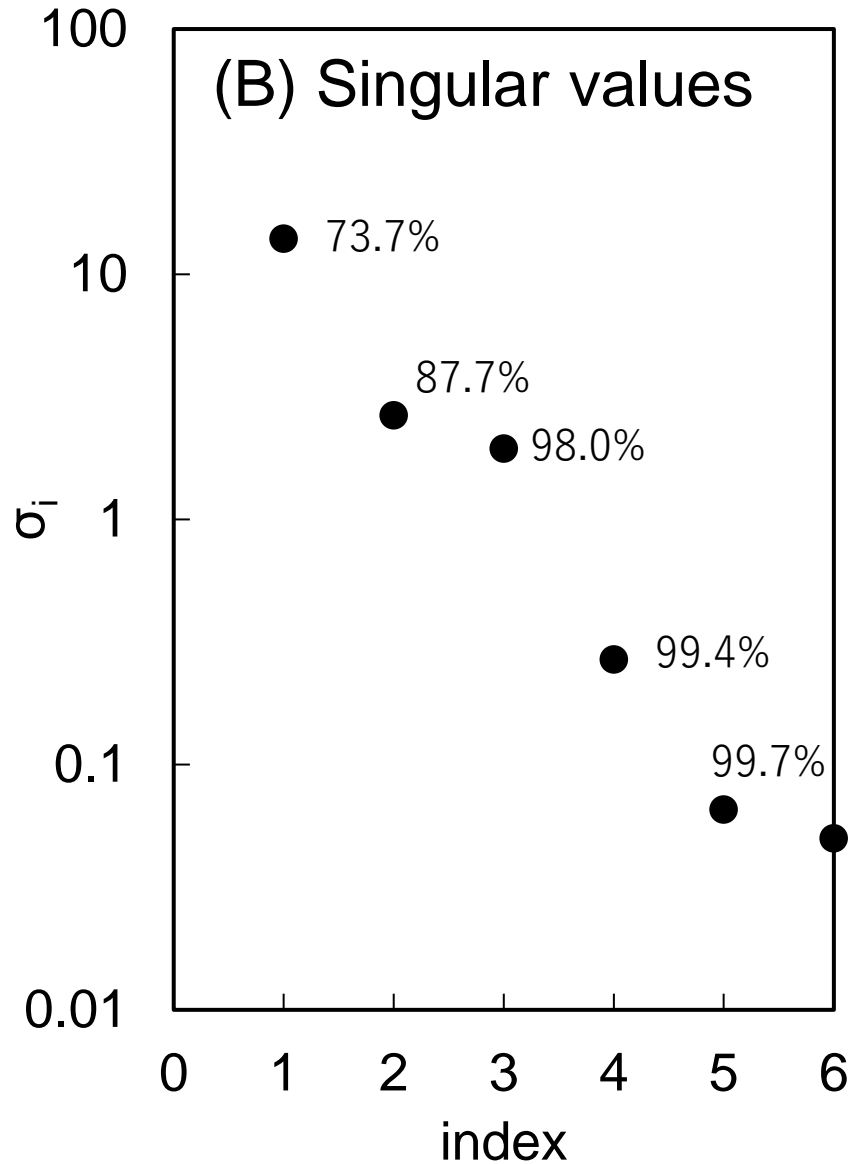


Figure S5 (B) Singular values and (C) basis functions for the first, second, and third compositions. The basis functions were extracted from the obtained spectra with the statistical intensity (variance) equivalent to the singular value of the corresponding index number.

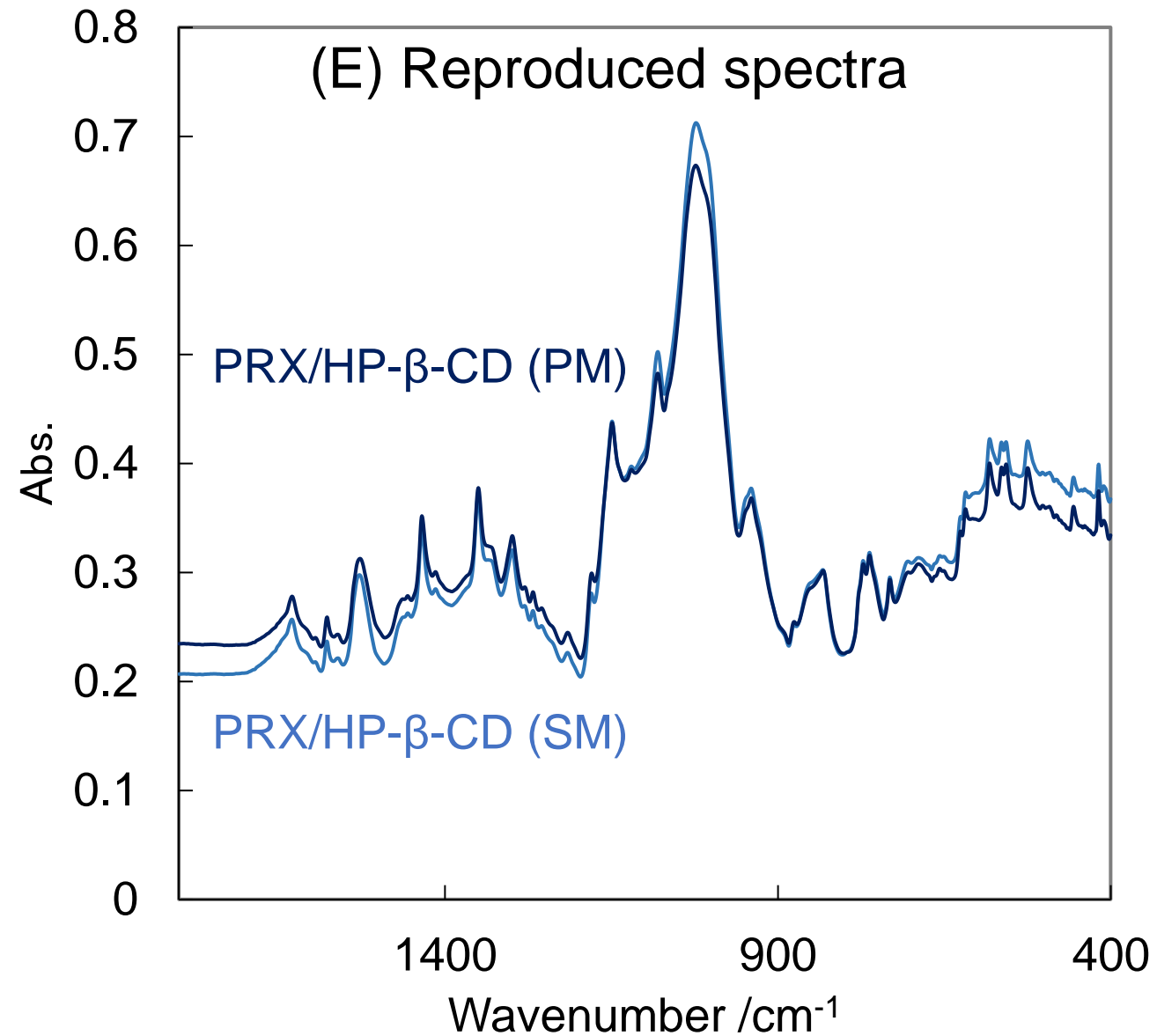
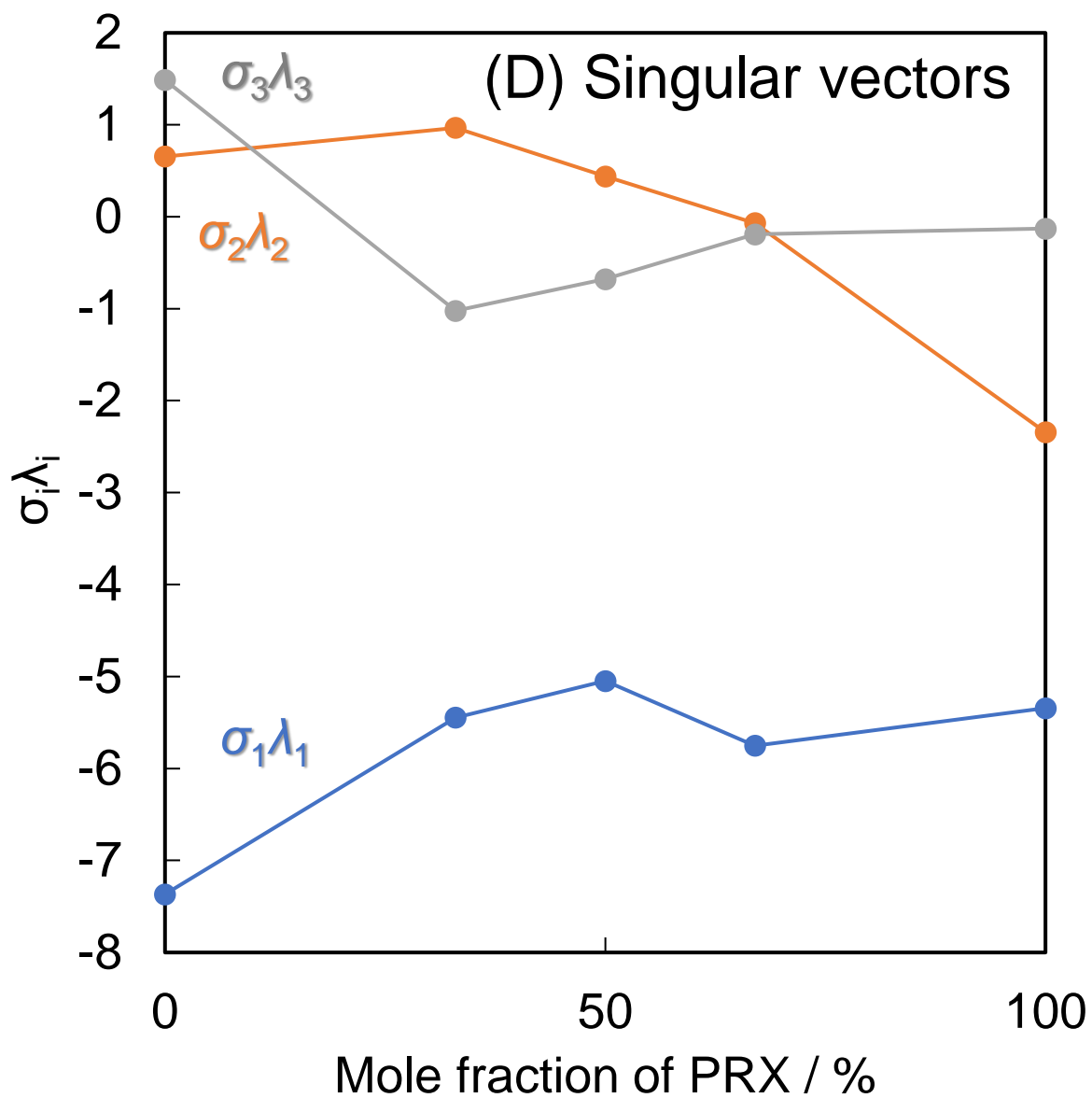


Figure S5 (D) Components of the first, second, and third singular vectors and (E) reproduced spectra of the PM- (indigo) and SM-prepared (blue) samples due to the linear combinations of 3 basis functions multiplied with the singular vector components.



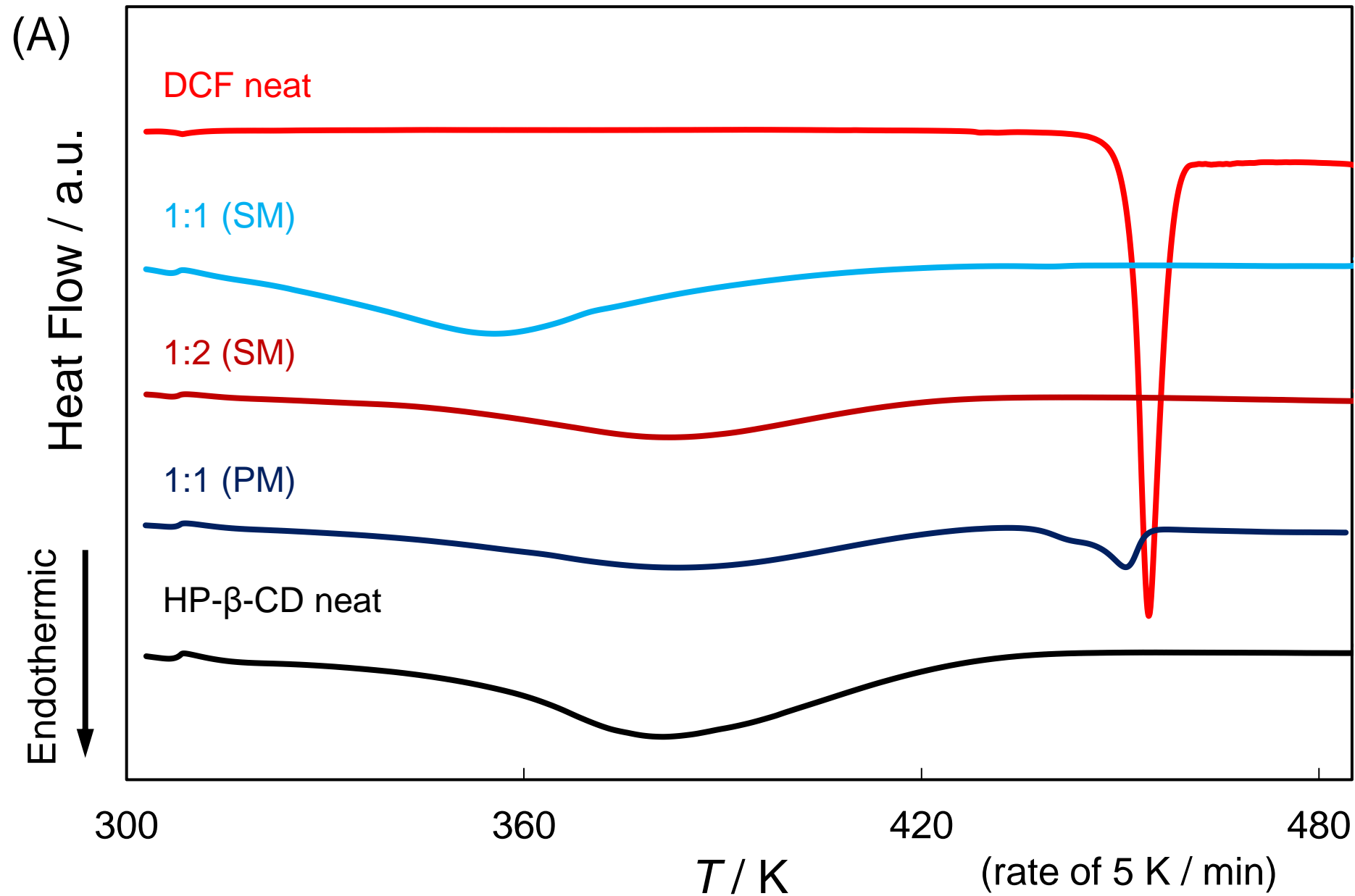


Figure S6(A).

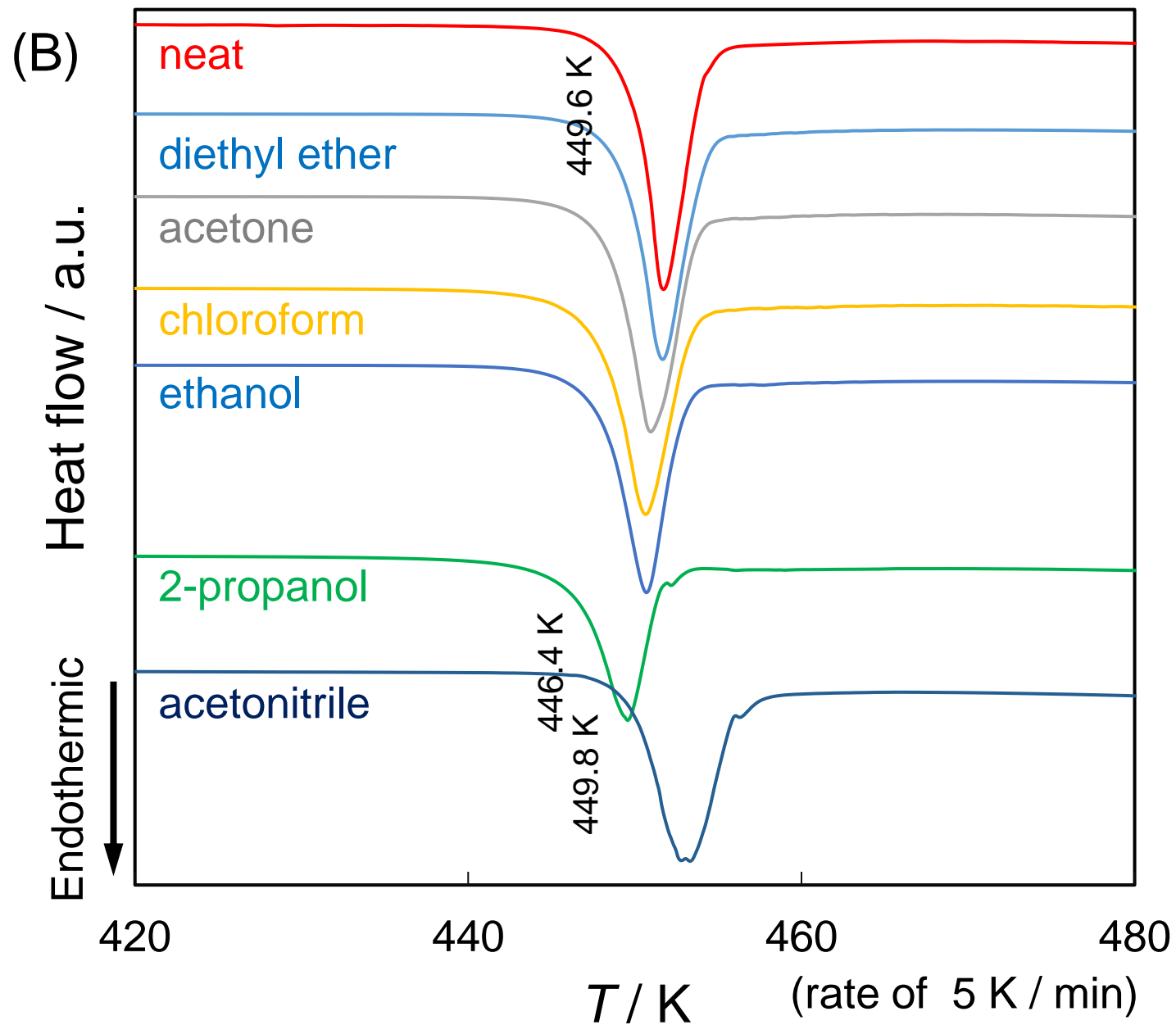


Figure S6(B) The DSC thermograms of the neat and various solvent-recrystallized DCF crystals.

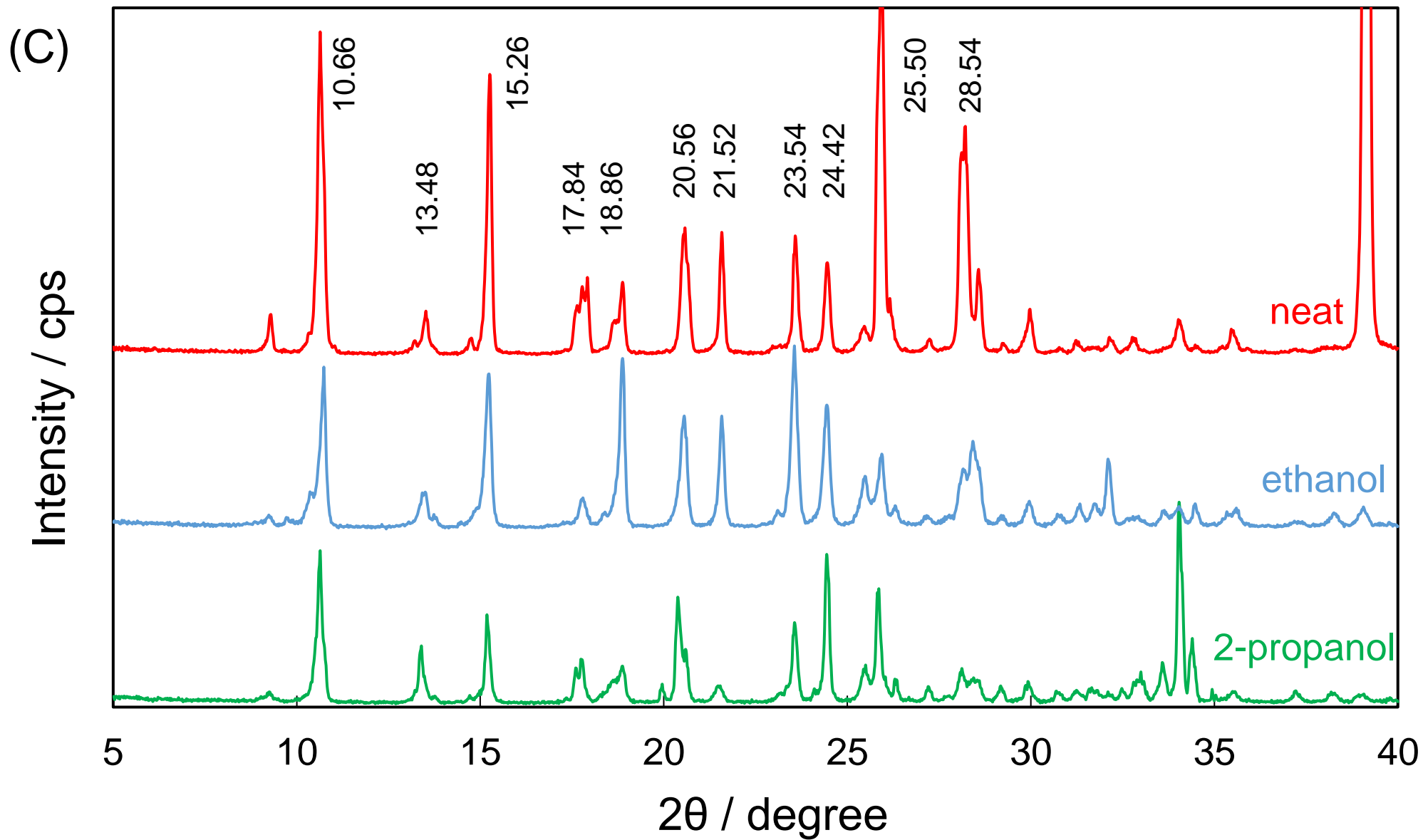


Figure S6(C) The XRPD patterns of the neat, ethanol-recrystallized, and 2-propanol-recrystallized DCF crystals. The  $2\theta$  values represent close to conspicuous peaks.

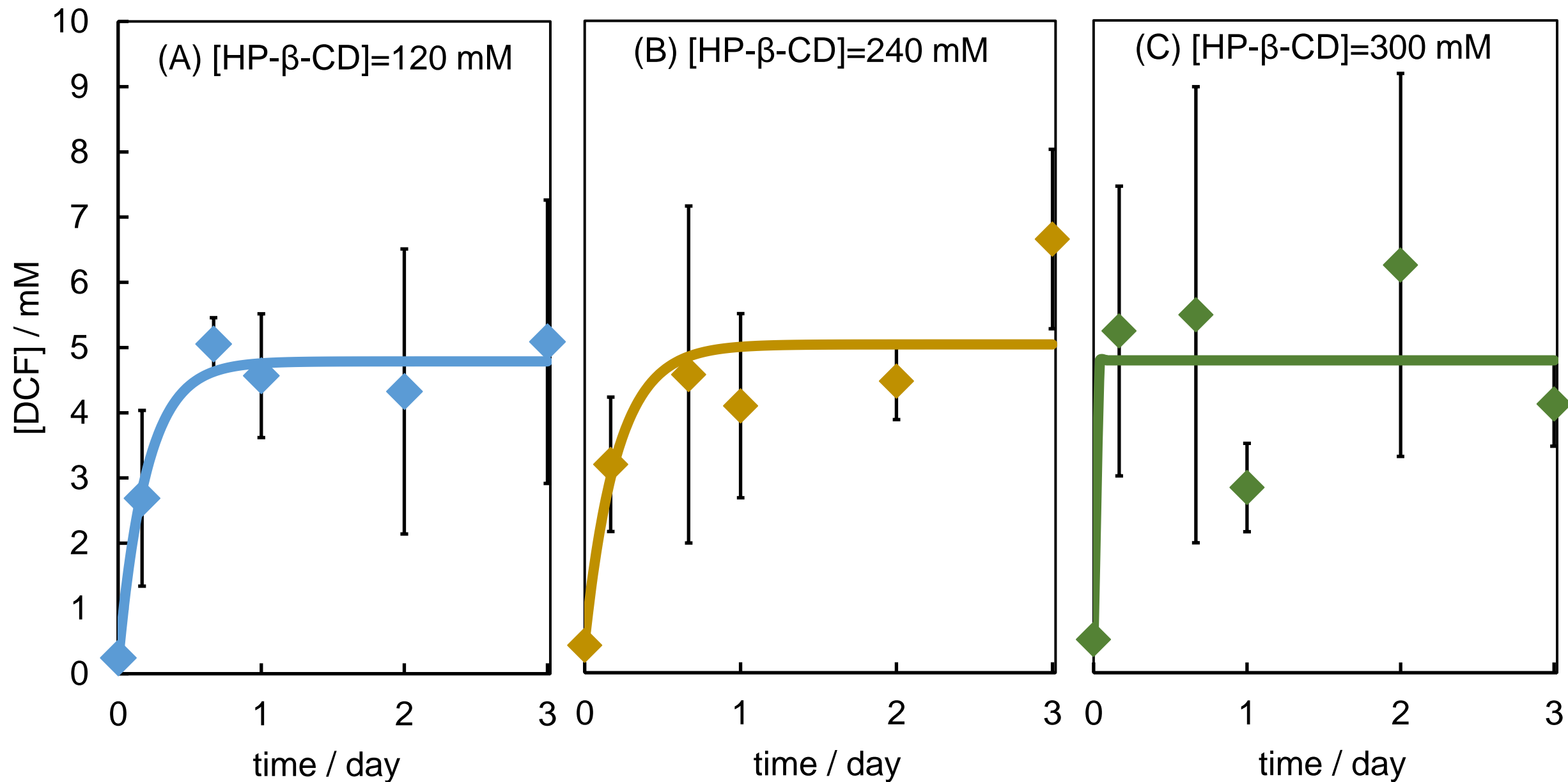


Figure S7 Dissolution curves of DCF in (A) 120 mM, (B) 240 mM, and (C) 300 mM HP- $\beta$ -CD aqueous solution. Reproducibility was secured with independent experiments of three times or more.

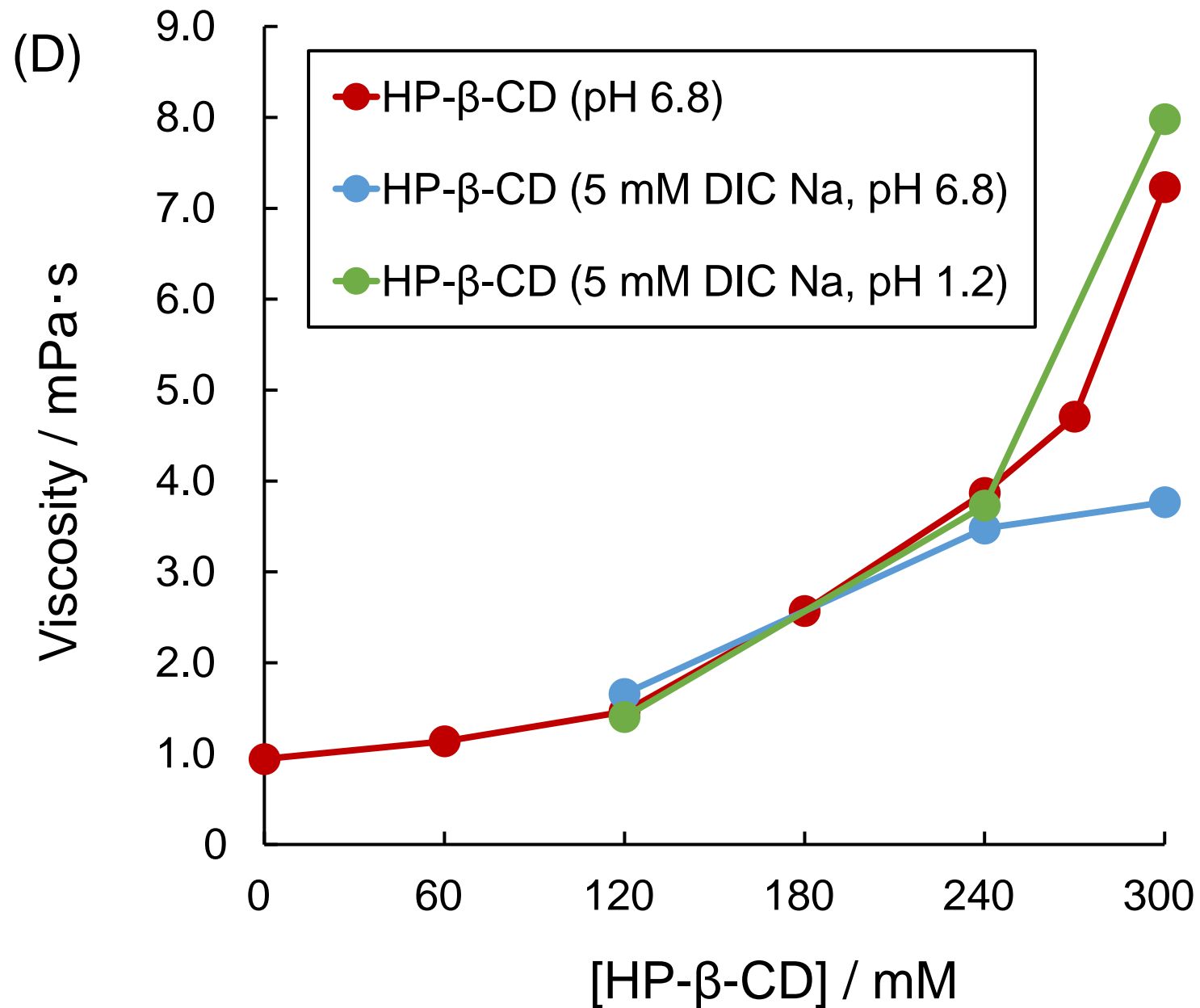
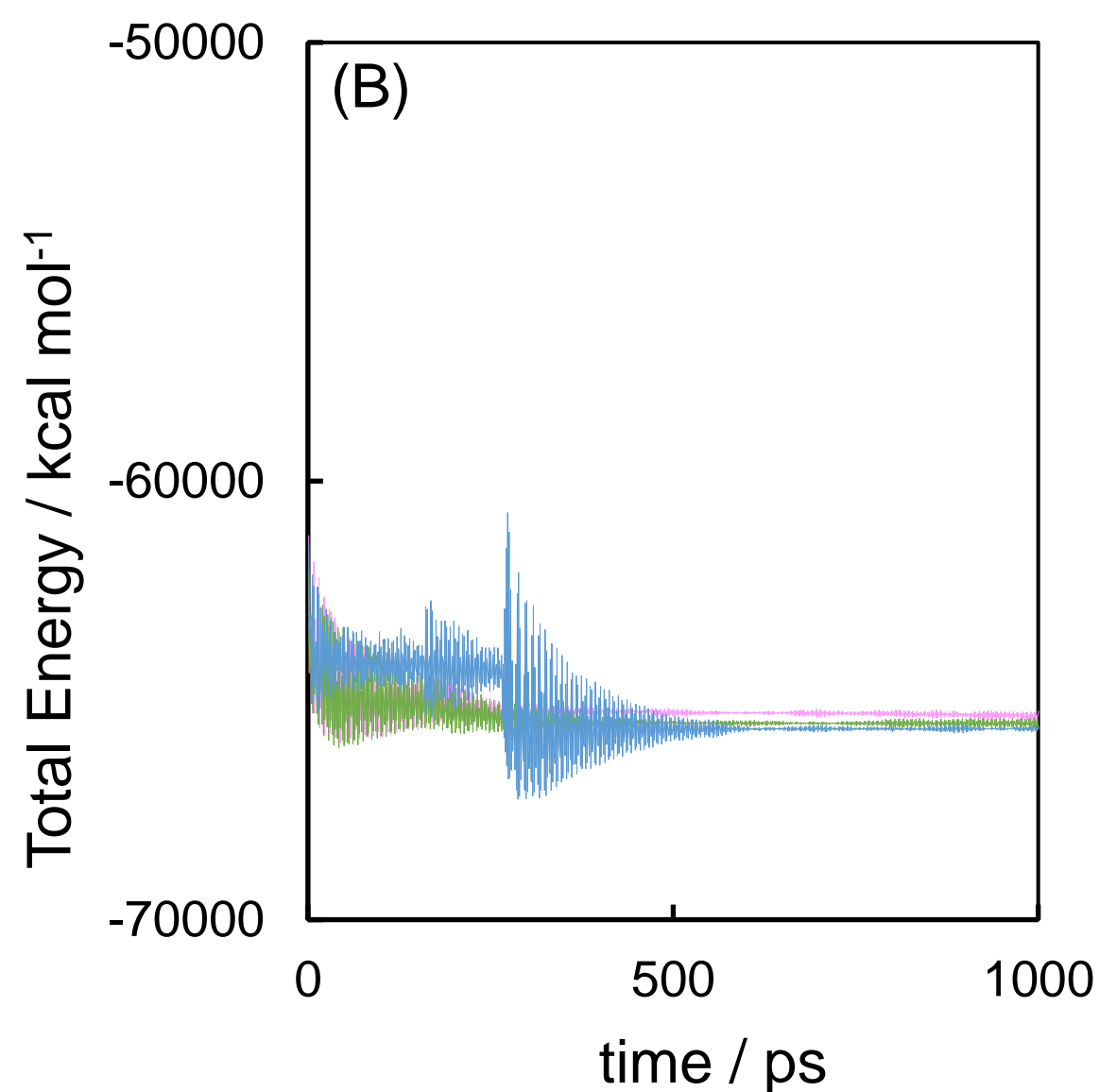
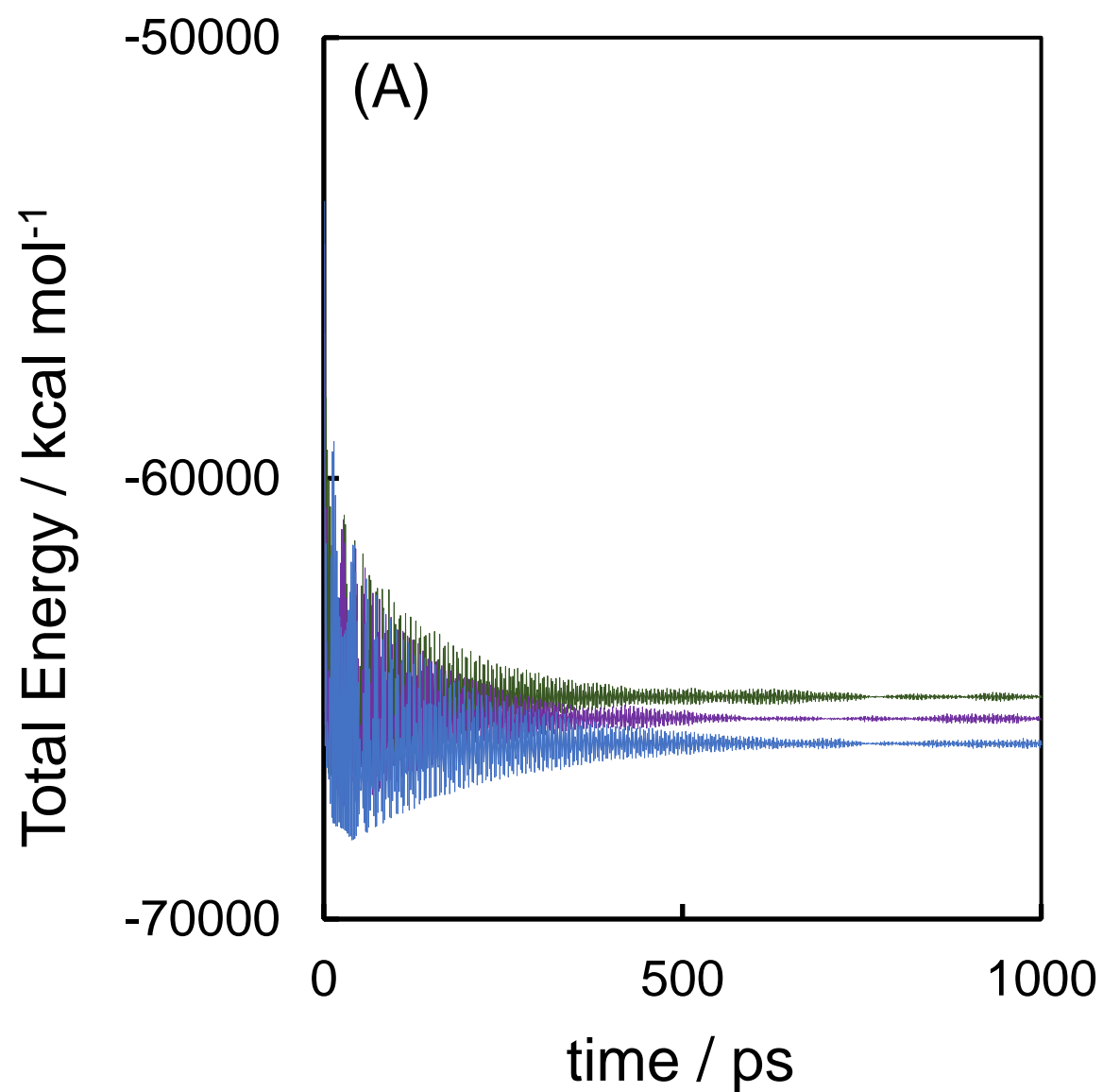


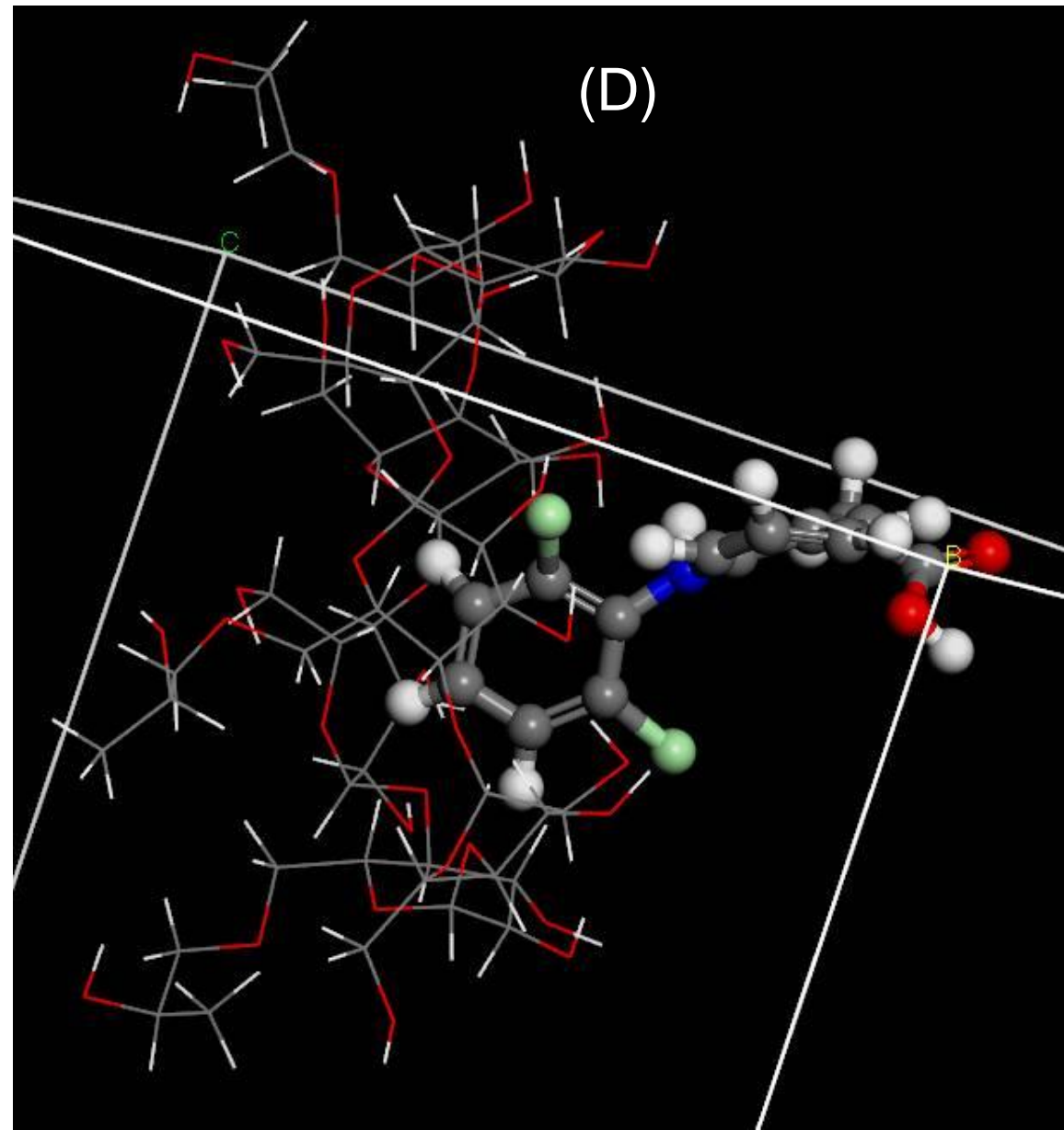
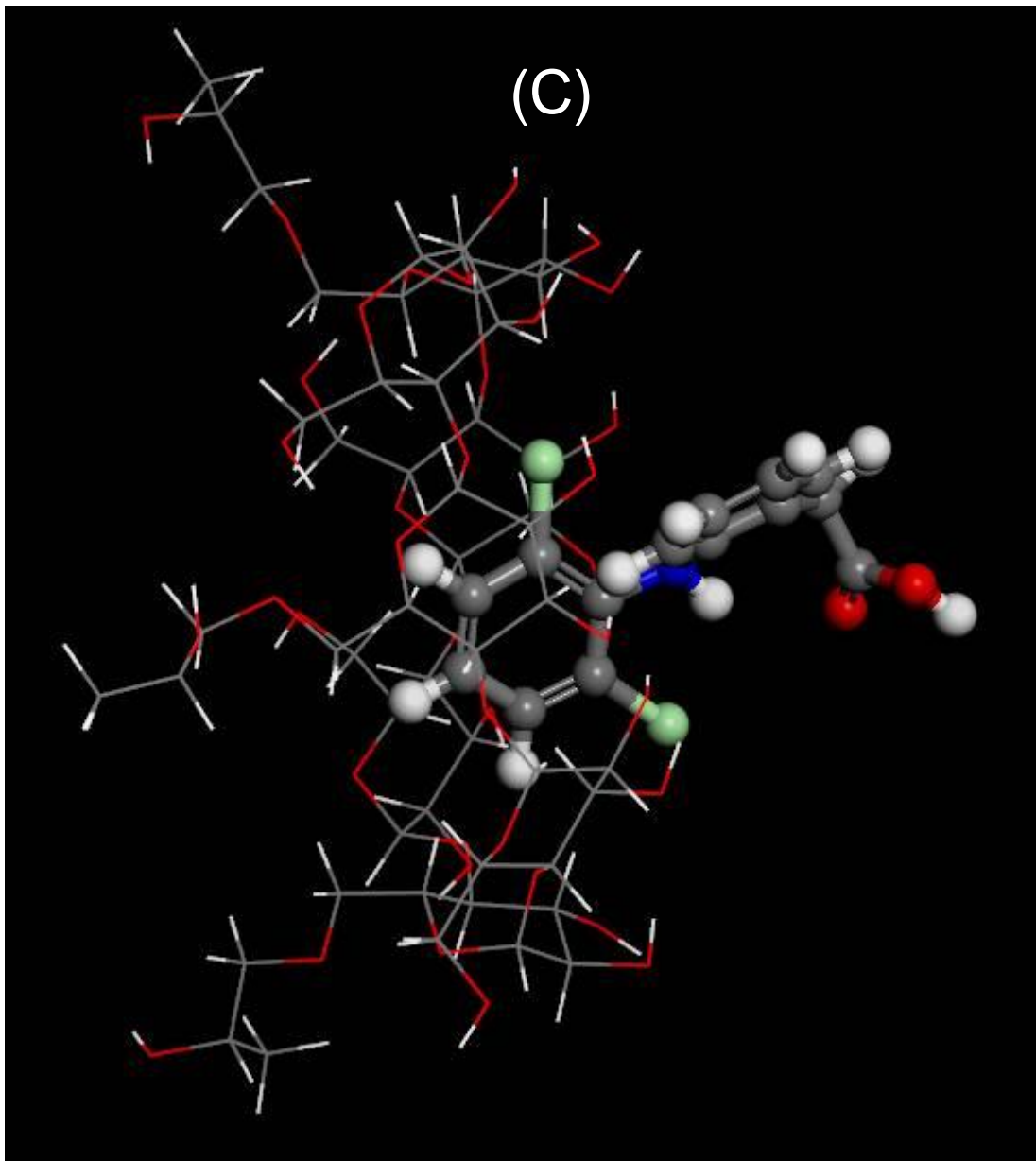
Figure S7(D) Viscosity versus HP-β-CD concentration in the presence and absence of 5 mM DCF at pH 6.8 and pH 1.2.

Table S1. The linear and parabolic approximations of phase-solubility diagram of INM, PRX, and DCF with HP- $\beta$ -CD.

	IND/HP- $\beta$ -CD	PRX/HP- $\beta$ -CD	DCF/HP- $\beta$ -CD
linear approximation	$0.0120x+4.44\times 10^{-6}$	$0.0457x+2.27\times 10^{-4}$	$0.00219x+2.96\times 10^{-5}$
$R^2$	0.9688	0.9855	0.9466
$D_0$	$4.44 \times 10^{-6}$	$2.27 \times 10^{-4}$	$2.96 \times 10^{-5}$
$K_{1:1}$	$2.67 \times 10^3$	211.	74.5
linear approximation	$0.0210x^2+0.66\times 10^{-2}x+4.44\times 10^{-6}$	$0.0616x^2+3.09\times 10^{-2}x+2.27\times 10^{-4}$	$0.0191x^2+1.69\times 10^{-4}x+5.31\times 10^{-5}$
$R^2$	0.9923	0.9992	0.9999
$D_0$	$4.44 \times 10^{-6}$	$2.27 \times 10^{-4}$	$5.31 \times 10^{-5}$
$K_{2:1}$	$1.49 \times 10^3$	136.	3.18
$K_{1:1}$	3.18	1.99	113.



Figures S8(A) and S8(B) Molecular dynamic trajectory of neutral (A) and anionic (B) DCF mixture with equimolar HP-β-CD. Whereas the neutral DCF was approached to 6-hydroxymethyl group side (dark green) and 2-/3-hydroxyl groups side (blue) and was isolated from HP-β-CD (violet), the anionic DCF was approached to 6-hydroxymethyl group side (green) and 2-/3-hydroxyl groups side (sky blue) and was isolated from HP-β-CD (pink)



Figures S8(C) and S8(D) Snap shots for stable and instable structures of the DCF/HP-β-CD complex.